

High-resolution studies of extreme-ultraviolet emission from CO by electron impact

Marco Ciocca*, Isik Kanik and Joseph M. Ajello

Jet Propulsion Laboratory, California Institute of Technology

Pasadena, California 91009

To be submitted to:

Physical Review A

PACSnumber(s): 34.80. Gs

May, 21996

* National Research Council Resident Research Associate

ABSTRACT

We report a high-resolution study [0.0036 nm fullwidth at half maximum (FWHM)] of electron-impact-induced emission spectra of CO at 30, 75 and 100 eV electron-impact energies. The spectral features were acquired in optically thin conditions, and represent the highest resolution single-scattering emission spectrum of CO induced by electron impact yet available. At the specified resolution, now attainable with our newly constructed 3-m vacuum ultraviolet spectrometer, we observe rotationally resolved emission bands of CO *in* the extreme-ultraviolet (euv), from the vibronic states B¹Σ⁺(0), C¹Σ⁺(0), and E¹Π(0), to the ground state X¹Σ⁺(0). A simple model of these bands, based on the Hönl-London factors and unperturbed rotational constants, is constructed and is shown to be in good agreement with the observed spectra. The predissociation yield for the E¹Π electronic state has been determined, showing that the E¹Π state has the largest predissociation cross section of CO for all singlet state Rydberg series members. The excitation function of the [E¹Π(0) ← X¹Σ⁺(0)] transition, in the 0-800 eV impact energy range, is measured for the first time, permitting determination of the oscillator strength by using a modified horn approximation analytical fit.

INTRODUCTION

As the most abundant interstellar molecule after H_2 [1], CO plays a very important role in the photochemistry of the interstellar medium (ISM) [2] . While H_2 , in most cases, cannot be detected directly, CO is readily observed by radioastronomy and therefore has been utilized as a tracer molecule [3] for molecular hydrogen. The abundance ratio of CO to H_2 is difficult to determine from observations of the ISM, but can be obtained through theoretical models [4] . These models involve chemical reactions in which photodissociation by vacuum ultraviolet radiation (vuv) is the main destruction mechanism for CO [1], particularly in the range between 91.2 nm, which is the edge of the absorption continuum of atomic hydrogen, and 111.8 nm, which is the dissociation limit of CO into ground state atoms. The rate of photodissociation of CO by vuv is one of the major uncertainties in these models. In view of these uncertainties and the importance of carbon monoxide as a tracer molecule, a large number of experimental studies have been performed. These studies were aimed at finding coincidences between molecular hydrogen emission lines and CO absorption lines, and at establishing the photodissociation rate in CO. A variety of techniques were used, including, classical spectrographs [5, 6], synchrotron radiation [7- 10], and laser methods [11-13]. A review of molecular parameters (wavelengths and oscillator strengths) of CO with comparison with uv data has been published recently [14]. It clearly points out that the large variation (a factor of 2) in the oscillator strengths of three of the strongest Rydberg states (B,C,E) of CO remain a major obstacle in modeling the ISM. These states have prominent (0,0) vibronic bands in the extreme ultraviolet (euv). For this reason, we have carried out the first high-resolution euv measurements of single-scattering excitation of the

rotational line structure by electron impact. We have recently reported [15] the oscillator strengths of the $B^1\Sigma^+(0) \rightarrow X^1\Sigma^+(0)$ and $C^1\Sigma^+(0) \rightarrow X^1\Sigma^+(0)$ transitions and, in this paper, we report the oscillator strength of the $[B^1\Pi(0) \rightarrow X^1\Sigma^+(0)]$ transition.

Of the dozen or more bound states in the singlet state manifold structure of CO, the B-state photoabsorption cross section dominates all discrete dissociation channels [10]. Photodissociation can occur, mainly, in two ways: either by continuum absorption into repulsive electronic states or via line absorption into predissociating states [16]. Experimental evidence [5, 10, 17] suggests that the latter mechanism is the more important for CO. In particular, line absorption into $ns\ \sigma, np\sigma^1\Sigma^+$ and $np\pi^1\Pi$ Rydberg series can be used to explain the absorption spectrum. Although the $3p\sigma C^1\Sigma^+(0)$ vibronic state has the largest absorption cross section in the euv [10], there is no evidence of either predissociation [10] or accidental predissociation [13]. The lowest energy predissociating state is the $3p\pi^1\Pi$. All Rydberg states for all Rydberg series above the $1:(0)$ vibronic level are 100% predissociated, as shown schematically in Fig. 1. The $1:(0)$ level is particularly interesting since it has the second largest absorption cross section in the euv [10] but is subject to only weak predissociation, as judged by the observed $B^1(0,0)$ band [15].

A comprehensive work on predissociation has been carried out recently using euv laser spectroscopy [12, 13, 18]. Predissociation reduces the lifetime of the excited state and may be detected as line broadening, which can affect the whole rotational manifold via direct coupling to the continuum or can affect a few rotational levels via accidental predissociation [12]. Laser spectroscopy studies for cases of strong predissociation have shown that the predissociation rates of CO can depend not only on which particular vibronic states are excited, but also on the

rotational substates and even on the A- doublet component of $^1\Pi$ states [18]. Because of the competition between radiative and dissociative channels, however, the fluorescence from predissociating states is reduced. Therefore, emission studies are a more sensitive probe of predissociation. As an example, in the medium resolution study of Ajello et al. [19], predissociation rates for the vibrational levels of the $c_4' \ ^1\Sigma_g^+$ state of N_2 , i. e. , the isoelectronic equivalent of CO, were so obtained, by comparing emission to excitation cross sections.

Our group at the Jet Repulsion Laboratory has also previously published both a low resolution [20] and medium resolution [15] studies of the electron impact-induced emission spectra of CO in the range 91-116 nm, showing transitions from the states $B^1\Sigma^+(0)$, $C^1\Sigma^+(0)$, and $F^1\Pi(0)$, to the ground state $X^1\Sigma^+(0)$. The internuclear distance for the minima in the potential curves of the Rydberg and valence states of CO overlies exactly at the minimum of the ground state, as shown in Fig. 1, resulting in intense (0,0) bands. In our earlier study [15], we reported the emission cross sections, together with a determination of the excitation function for the $B(O, O)$ and $C(O, O)$ transitions. Oscillator strengths for these transitions were also reported [15]. At the spectral resolution under which those spectra were obtained [FWHM = 0.025 nm], it was not possible to observe the rotational line-structure of the transitions in question. In search for the rotational substates dependence of predissociation rates for weak predissociation, in this high-resolution study, complementary to the laser spectroscopy, we present the CO emission spectra for the $B(0)$, $C(0)$ and $F(0)$ states. With a FWHM of 0.0036 nm, it is now possible to resolve the rotational structure of the $F(0, O)$, $C(O, 0)$ and $B(0, O)$ transitions. In addition, the excitation function for the $F^1\Pi(0) \rightarrow X^1\Sigma^+(0)$ band has been measured for the first time. By fitting the

shape of the excitation function with an analytical expression based on the modified Born approximation [21, 22], the oscillator strength has also been determined

In the remainder of this paper, we describe the experimental apparatus, the high resolution measurements of the (0,0) resonance transitions of the B,C,E states and the spectroscopic model, and finally the measurement of the 1{(0,0) excitation function and modified Born approximation analysis.

EXPERIMENTAL APPARATUS

The experimental apparatus has been described in detail elsewhere [23]. in brief, a high-resolution 3.0-m spectrometer system was used. It consists of an electron impact collision chamber in tandem with a uv spectrometer. UV emission spectra of CO were measured by crossing a magnetically collimated beam of electrons with a beam of CO gas. A Faraday cup, designed to minimize detection of backscattered and secondary electrons, is used to monitor the electron current.

To acquire emission spectra, the beam of CO, formed by a capillary array, is crossed by an electron beam at 90°. The impact-energy of the electron beam is kept fixed and emitted photons, corresponding to radiative decay from the collisionally excited states of CO, are dispersed by the uv spectrometer and then detected by a channeltron detector. A resolving power of $\lambda/\Delta\lambda \cong 30,000$ was achieved by operating the spectrometer in second order, with both entrance and exit slits equally set at 20 μ m. The slit function at this setting was triangular, with a

resolution of 0.036 Å FWHM. The emission spectra were obtained at various incident electron energies. In particular, spectra were obtained at 30 eV for the B(0,0) transition, 75 eV for the D(0,0) and 100 eV for all the bands.

Excitation function measurements for the D(0) state were carried out at a specific wavelength (1076.1 Å) by measuring the relative intensity of the emitted radiation as a function of the electron beam energy. In this case a uniform static sample of CO was admitted to the chamber, forming a cylindrical line-source collision region, thereby eliminating problems associated with a possible variation in size of the electron beam with changing energy.

All transitions observed in this study are toward the ground state of CO, X¹Σ⁺(0) and therefore, to ensure optically thin spectra, care must be taken in choosing the operating pressure. If the optical depth at line center of the strongest rotational lines is less than 0.1, self absorption effect can be neglected. Below this pressure the measured cross section will be independent of pressure. The procedure used to determine the maximum background pressure that can be used and while maintaining optically thin conditions has been presented in detail elsewhere [15]. The photon path length from the interaction region to the entrance slit of the spectrometer was 11.0 cm and the laboratory apparatus temperature was 330 K (due probably to radiative heating from the hot filament in the electron gun). In this case, optically thin conditions were achieved by maintaining a background gas pressure in the collision chamber of less than 4.0 × 10⁻⁵ Torr for the D- state and less than 1.0 × 10⁻⁵ Torr for the B- and C-state.

EXPERIMENTAL RESULTS

The measurements described here involve highly excited states of CO. A schematic potential energy diagram (in which the states studied are indicated), is presented in Fig. 1. The shaded area indicates the Franck-Condon region. The high resolution, electron-impact emission spectra of $B^1\Sigma^+(0) \rightarrow X^1\Sigma^+(0)$, $C^1\Sigma^+(0) \rightarrow X^1\Sigma^+(0)$ and $B^1\Pi(0) \rightarrow X^1\Sigma^+(0)$ transitions are in the 1070-1160 Å region, and are shown in Figs. 3, 4, 5, and 6. Figure 3 gives an overview of all the features of the emission spectrum of CO studied in this work, with identifications. The spectra were obtained at 100 eV electron-impact energy, with a background gas pressure of 1.0×10^{-6} Torr, in order to avoid effects of self-absorption, especially for the $C^1\Sigma^+ \rightarrow X^1\Sigma^+(0)$ band, which has the largest oscillator strength of the three bands studied [15].

The spectral region from 1075.4 to 1077.5 Å contains the direct transition from the $B^1\Pi(v' = 0)$ to the ground state, while the region from 1086.5 to 1088.5 Å shows the rotationally resolved transitions from the $C^1\Sigma^+(0)$ again to the ground state of CO. The $C^1\Sigma^+$ state has been the subject of numerous spectroscopic investigations. The first was performed by Hopfield and Birge [24]. Recently, Feldberg et al. [5, 6] performed an absorption study of this state in the VUV, while an extensive study employing emission laser spectroscopic techniques has been reported by Ubachs et al. [13]. In the 1149.5 to 1151.5 Å spectral region, we observe the emission transition from the $B^1\Pi(0)$ excited state of CO to the ground state and an atomic component ($O^1D - ^1D^0$) at 1152.15 Å [25]. The $B^1\Pi(v') \rightarrow X^1\Sigma^+(v'')$ vibronic bands have been studied in detail by Feldberg et al. [26], both in absorption and in emission. The emission spectrum was obtained by means of a discharge lamp, with a CO pressure of few millitorr. They observed

predissociation for the $B(v = 1,2)$ levels but no predissociation in the $B^1\Sigma^+(0) \rightarrow X^1\Sigma^+(0)$ band. As reported by Kanik et al. [15], this band exhibits an anomalous behavior, showing a sharp peak in the excitation function at very low electron-impact energies, probably arising from spin exchange due to significant triplet admixture [15]. For this reason, we obtained a spectrum of the $B^1\Sigma^+(0,0)$ transition at an electron-impact energy of 30 eV, which corresponds to the maximum of the emission cross section for this state [15]. The results are presented in Fig. 4, where the individual J levels up to $J=19$ for the R-branch are clearly resolved. In this figure we also compare the measured spectrum with the output of a model, which will be described in detail below.

The model, based on the Hönl-London factors, makes use of the unperturbed rotational constants of Ubachs et al. [18] (Table 1) for this state, and of Huber and Herzberg [27] for the ground state. The model generates emission intensities and wavelengths for the rovibronic transitions from the excited state to the ground state. One of the parameters of the model is the temperature of the gas sample. It was found that the best agreement between data and model was achieved by adopting a temperature value of 330 K. By convoluting the model intensities with the triangular slit function of the spectrometer, we obtain a synthetic spectrum that can then be compared with the measured spectrum. The model output and the data are both normalized to unity, to facilitate comparison. We obtain a good agreement, as shown in Fig. 4. The triplet-state admixture does not seem to affect the singlet character of the state to any great extent. It is quite clear that no perturbations are present in the experimental data, and that the model fits

satisfactorily. It must be pointed out that no predissociation can be found from the $B^1\Sigma(v=0)$ state, since it lies below the dissociation limit of CO.

In Fig. 5 we present a spectrum of the $C^1\Sigma^+(0) \rightarrow X^1\Sigma^+(0)$ transition. The energy of the $C^1\Sigma^+(v=0, 1)$ levels lies above the dissociation limit, 11.09 eV, so that they may either predissociate or decay via fluorescence (see Fig. 1). Letzelter et al. [10] reported that the predissociation yield of the C(0) level is at the most 10%, while the C(1) is almost entirely predissociated. The $C^1\Sigma^+(0) \rightarrow X^1\Sigma^+(0)$ transition, shown in Fig. 5, contains approximately 98% of the cuv emission between the $C^1\Sigma^+$ state and the ground state [20 and ref. therein]. Here again our model (which does not contain any predissociation terms in this case) is in good agreement with the observed spectrum, thus indicating that almost no perturbation or accidental predissociation is present.

In Fig. 6 we show the spectrum of the $B^3\Pi(0) \rightarrow X^1\Sigma^+(0)$ transition, again compared with the model output (this time with a predissociation term). This transition was first observed by Hopfield and Birge [24] in emission. This led to the conclusion that the level $B^3\Pi(0)$ was not predissociated. Lee and Guest [17], however, found very weak fluorescence from this state and Letzelter et al. [10] were able to determine that the $B^3(0)$, although still fairly intense in emission spectra, was indeed predissociated. This was determined with a measurement of the fluorescence yield after excitation by synchrotron radiation. An accidental predissociation of the $B^3(0), J=3$ level of c-parity was observed by Simmons and Tilford [28]. Baker et al. [29] identify the perturber as the $k^3\Pi(v=3), J=3$ level. In their extensive laser spectroscopy study

at high temperature, Cacciani et al. [12] also observed accidental predissociation for two more J levels ($J_e=41$ and $J_e=44$), and assigned the perturber as the $k^3\Pi(v=4)$ state.

PREDISSOCIATION YIELD FOR $E^1\Pi(O)$

To determine the predissociation yield of this state, we have used an alternative and entirely different approach which generates complementary information to the UV emission process: electron impact excitation. For example, for states with negligible or known cascading branching, predissociation cross section can be obtained by comparing the measured emission cross section from that state to the corresponding excitation cross section obtained from the electron energy-loss spectrum. The predissociation cross section E-state of CO (where cascade contribution is zero) may be estimated using the following expression:

$$Q_{pre} = Q_{exc} - (Q_{emis} + Q_b) \quad (1)$$

where Q_{pre} is the predissociation cross section, Q_{exc} is the direct excitation cross section, Q_{emis} is the emission cross section of an electronic state (in our case $E^1\Pi$) to the ground state ($X^1\Sigma^+$) and Q_b is the “branching” cross section. In eqn. 1., the quantity $Q_{emis} + Q_b$ represents the “total” emission cross section. After the initial excitation the CO molecule can branch down through several intermediate states and produce fluorescence in the wide range of wavelengths, in addition to the direct UV transition to the ground state measured in this work. This approach has been used for the determination of predissociation yields of the c_4' , b' and b states of N_2 [19, 30] and 11_2 Rydberg states [31].

For a negligible or known amount of cascading from an upper state (and/or branching to a lower state), the total emission yield of an excited electronic state i to the ground state x can be defined as

$$(\eta_E)_{i \rightarrow X} = \frac{Q_{emis}}{Q_{exc}} \quad (2)$$

The predissociation yield, η_p , for an excited electronic state of CO may then be estimated using the following expression:

$$\eta_p = 1 - [(\eta_E)_{i \rightarrow X} + \sum_k (\eta_E)_K] \quad (3)$$

where $\sum_k (\eta_E)_K$ represents the total emission yield of an excited state to all lower excited electronic states (i.e. branching) other than the ground state. The branching ratio estimates indicated that branching loss from the $B^1\Pi^1$ state, via $B^1\Sigma^+$, $C^1\Sigma^+$ and $A^1\Pi$ states, accounts for a maximum of only 8% of the total emission observed from the $B^1\Pi^1$ state [20].

By employing equations (2) and (3), we obtain an amount of 88% predissociation yield for the $B^1\Pi^1$ electronic state based on the comparison of direct excitation [32] and total emission [15] cross sections and taking into account of 8% emission yield to lower excited states ($B^1\Sigma^+$, $C^1\Sigma^+$ and $A^1\Pi$). Ietzelter et al. [10] measured predissociation yield for individual vibrational states ($v' = 0$ and $v' = 1$) of the $B^1\Pi^1$ electronic state and found 89% and 98% predissociation, respectively. The two measurements for the $B^1\Pi^1(v' = 0)$ state are found to be in excellent agreement.

In the next section, we will present our model of the $E(0,0)$ transition. This model and the data presented in Fig. 6 allows us to obtain predissociation yields for the $11'$ and $11''$ sublevels of the $E(0)$ level.

THE MODEL,

The present measurements of the rotational line intensities of the $COB(0,0)$, $C(0,0)$ and $11'(0,0)$ transitions were modeled by use of Hönl-London factors. The construction of the model for producing synthetic spectra for $\Sigma-\Sigma$ and $\Sigma-\Pi$ transitions has been described in detail elsewhere [23, 31]. Strong perturbations can be neglected, except for weak predissociation of the $ii(O)$ vibrational level by an unknown repulsive predissociating state(s). The results are in stark contrast to our recent work on EUV transitions for the isoelectronic molecule N_2 [33], in that work, analysis of the $N_2(c_4'(0,0))$ was performed and demonstrated that the rotational envelope of the Carroll-Yoshino resonance band shows evidence of strong perturbations by several nearby states.

A brief description of the CO model is given below. The excitation and emission fine structure transitions for $\Sigma-\Sigma$ and $\Sigma-\Pi$ are shown schematically in Fig. 2. The measured intensity, I , of any rotational line (J, J'') is proportional to the excitation rate. The excitation rate, $g(v', J)$ to any upper rotational level J is given by

$$g(v', J) = Q_{v'} F \sum_{J''=J-1}^{J''=J+1} \left[\frac{N(v'', J'') S(J, J'')}{(2J'' + 1)} \right] \quad (4)$$

where $Q_{v'}$ is the excitation cross section, F is the electron flux, $N(v'', J'')$ is the population in the ground level and S is the normalized Hönl-London line strength [31]. The rotational line intensities for the P ($J'' = J + 1$) and R ($J'' = J - 1$) branches of the $11(0,0)$ and $C(0,0)$ rovibronic transitions are given by:

$$I_{v'v'', JJ''} = g(v', J) \omega_{v'v'', JJ''} \quad (5)$$

where $\omega_{v'v'', JJ''}$ is the branching ratio, given by

$$\omega_{v'v'', JJ''} = \frac{A_{v'v'', JJ''} S(J, J'')}{\sum_{v''} A_{v'v'', JJ''} S(J, J'')} \quad (6)$$

where $A_{v'v''}$ is the spontaneous emission transition probability for the (v', v'') band (in our case we limit ourselves to the $v' = v'' = 0$ case), $\sum_{v''} A_{v'v''}$ is the total emission transition probability for all

lower vibrational levels v'' , given by $\sum_{v''} A_{v'v''}$.

in order to reproduce, however, the measured spectrum of the $11(0,0)$ band (Fig. 6), the emission branching ratio must have a term which depends on the effects of predissociation. In this case, we write

$$\omega_{v'v'', JJ''} = \left[\frac{A_{v'v'', JJ''}^+ S(J, J'')}{\sum_{v''} A_{v'v'', JJ''}^+ S(J, J'')} \right] \eta_E(v', J) \quad (7)$$

where $A_{v'v'', JJ''}^+$ is the spontaneous emission transition probability of the 11^+ (the P and R branches) state, assumed to be constant in J for any v' , and analogously for the 11^- state (Q branch) and

$\eta_E(v', J)$ is an emission yield, given by:

$$\eta_{E}^{+}(v', J) = \frac{A_{v'}^{+}}{A_{v'}^{+} + A_{pre}^{+}(v', J)} \quad (8)$$

where $A_{v'}^{+} + A_{pre}^{+}(v', J)$ is the total transition probability, and includes the predissociation transition probability, $A_{pre}^{+}(v', J)$, for any $E(0)$ rotational level J .

The rotational line intensities then become:

$$I_{v'v'', JJ''}^{+} = g(v', J) \frac{A_{v'v''}^{+} S(J, J'') \eta_{E}^{+}(v', J)}{v' A_{v'}^{+}} \quad (9)$$

and similarly for the Π^{-} state. The data for the $E(0, 0)$ transition, shown in Fig. 6, suggest that $\eta_{E}^{+}(J)$ and $\eta_{E}^{-}(J)$ are to a good approximation independent of J , although different for the Π^{+} and Π^{-} states, since no sudden weakening of the band is observed, in agreement with observations by Cacciani et al. [12]. This yield can then be represented by constants η_{E}^{+} and η_{E}^{-} . The experiment uniquely determines the ratio between these two yields, since the spontaneous emission probabilities for the Π^{+} states and Π^{-} states are independent of J for negligible perturbation with other bound states. The Π^{+} and the Π^{-} emission yields are related to the total emission yield by

$$\frac{\eta_{E}^{+}}{2} + \frac{\eta_{E}^{-}}{2} = (\eta_{E})_{i \rightarrow X} \quad (10)$$

in the high temperature limit ($T \geq 300$ K). The emission model for the $E(0, 0)$ transition, when we assume equal predissociation for the Π^{+} and Π^{-} sublevels, overestimates the brightness of the Q-branch. The experimentally determined ratio between the emission yields of

the $11'$ and $11''$ sublevels is equal to $\eta_{E^-} / \eta_{E^+} = 0.63$. Using this ratio, and eqn. (10), we obtain $\eta_{E^+} \approx 0.135$ and $\eta_{E^-} \approx 0.085$. From eqn. 3, then, it finally follows that the predissociation yields for the $11'$ and $11''$ sublevels (η_p^+ and η_p^- , respectively) are $\eta_p^+ = 0.85$ and $\eta_p^- = 0.91$.

Although it is clear from the present measurements that the $B^1\Pi$ state predissociates, the electronic continuum states causing this perturbation are yet to be determined. A list of candidate predissociating states can be found by considering the ways the $C(^3P)$ and $O(^3P)$ atoms can join angular momenta along the internuclear axis. The possible singlet states are $^1\Sigma^+$, $^1\Sigma^-$, $^1\Pi$ and $^1\Delta$ [34]. According to the selection rules for predissociation, only transitions to like-parity states can occur. Therefore a repulsive $^1\Sigma^-$ state may be responsible for the enhanced predissociation of the 11^- state observed in this experiment.

OSCILLATOR STRENGTHS

Previous experimental and theoretical determinations of oscillator strengths $f_{v',v''}$ from $v'' = 0$ of the $X^1\Sigma^+$ ground state of CO to different v' levels of the $B^1\Sigma^+$ and $C^1\Sigma^+$ states have been summarized in our earlier paper [15]. In this paper, we report the oscillator strength for the $B^1\Pi(v' = 0) \rightarrow X^1\Sigma^+(v'' = 0)$ transition and compare it with other data sets where available.

We obtain the oscillator strength for the $B^1\Pi(v' = 0) \rightarrow X^1\Sigma^+(v'' = 0)$ transition by analyzing the energy dependence of the measured excitation function (from 0 to 800 eV) corresponding to that transition. The excitation function for the $B^1\Pi(v' = 0) \rightarrow X^1\Sigma^+(v'' = 0)$ transition (Fig. 7) is put on an absolute scale by normalizing it to the 100 eV excitation cross

sections for the $\text{CO}^1\Pi(v' = 0) \rightarrow \text{X}^1\Sigma^+(v'' = 0)$ transition [32]. From eqn. (1), the predissociation, emission, excitation and branching cross sections at 100 eV are then obtained, and are reported in Table 1 I.

Collision strength data (cross section times electron impact energy) for the $\text{CO}^1\Pi$ band were fitted within experimental error (about 20%) using the following analytical form for collision strength:

$$\Omega_{v'v''}(X_{v'v''}) = C_0 \cdot (1 - 1/X_{v'v''}) \cdot (X_{v'v''})^2 + \sum_{k=1}^4 C_k \cdot (\sim V'V'' - 1) \cdot \exp(-k \cdot C_8 X_{v'v''}) + C_5 + C_6 / X_{v'v''} + C_7 \cdot \ln(X_{v'v''}) \quad (11)$$

where $\Omega_{v'v''}(X_{v'v''})$ is the collision strength, $X_{v'v''}$ is the electron impact energy in threshold units, and C_k are constants of the function $\Omega_{v'v''}(X_{v'v''})$ [21, 22]. The result of this fit is reported in Fig. 5. The constant C_0 represents the contribution of electron exchange, $C_1 - C_4$ represent configuration mixing, $C_5 - C_6$ represent polarization effects, C_7 is the Born term and C_8 is a constant in the mixing terms. Table 111 gives the constants of eqn. (11) for the $\text{CO}^1\Pi(v' = 0) \rightarrow \text{X}^1\Sigma^+(v'' = 0)$ transition. The excitation cross section is given by the equation

$$\sigma_{v'v''}(X_{v'v''}) = \Omega_{v'v''}(X_{v'v''}) \cdot (E_{v'v''} \cdot X_{v'v''})^{-1}, \quad (12)$$

where $\sigma_{v'v''}(X_{v'v''})$ is the cross section in atomic units, and $E_{v'v''}$ is the transition energy in Rydberg units. At the high energy limit the collision strength has the following form:

$$\Omega_{v'v''}(X_{v'v''}) \approx C_5 + C_7 \cdot \ln(X_{v'v''}), X_{v'v''} \gg 1 \quad (13)$$

In the Bethe Approximation [35], the collision strength is given by

$$\Omega_{v'v''}(X_{v'v''}) = \omega_{v''} \left(\frac{8ma_0^2}{h^2} \right) \frac{f_{v'v''}}{E_{v'v''}} (\ln X_{v'v''} + 4C_{v'v''} E_{v'v''}) \quad (14)$$

where $\omega_{v''}$ is the lower state degeneracy, $C_{v'v''}$ is a constant, related to the angular distribution of the scattered electrons, $f_{v'v''}$ is the oscillator strength, a_0 is the Bohr radius, m is electron mass, and h is the Planck's constant, Thus

$$C_7 = \omega_{v''} \left(\frac{8ma_0^2}{h^2} \right) \frac{f_{v'v''}}{E_{v'v''}} \quad (15)$$

As seen in Eqn. (15), the optical oscillator strength can be related to one of the constants in the fitting function at the high energy limit. This equation allows us to determine the oscillator strength. For the $CO: {}^1\Pi(0) \rightarrow X^1\Sigma^+(0)$ transition the optical oscillator strengths was found to be 7.08×10^{-2} . The experimental collision strength and the analytic fitting function for the $CO: {}^1\Pi(0) \rightarrow X^1\Sigma^+(0)$ transition are shown in Fig. 8. The error associated with the oscillator strength is estimated as follows: (a) 26% error from the $CO: X \rightarrow {}^1\Pi$ excitation cross section [32] and (b) So/O error from the fitting procedure. Thus the overall error (square root of the sum of the squares of the contributing errors) in the oscillator strength is estimated to be about 26%. Some discrepancies, in the threshold region (10-15 eV), between the analytical fit and the data are

present, requiring further studies. The determination of the oscillator strength, however, relies on the fit at high energy, which is completely satisfactory,

Since there is no cascading into the $F(0)$ state, we can assume that the energy variation of the excitation, predissociation, mission and branching cross sections is the same. From the analytical fit of the excitation function and by using eq. 1, we then obtain analytical fits to the predissociation and branching (as stated earlier, branching to lower excited states is 8% of the total emission) cross sections, shown in Fig. 9, in the 0-500 eV range. Also shown are excitation and emission cross sections.

There are many reported experimental and theoretical data for the oscillator strength of the $F(0)$ state. Table IV summarizes the oscillator strength values obtained by different researchers for the $COF(0) \rightarrow X^1\Sigma^+(0)$ transition. Large variations exist among these values. A comparison of the oscillator strengths gives an excellent agreement between the present result and that of Chan et al. [36] (disagreement is less than 1%). There is also a fair agreement between the data of Lassette et al. [37] and the present value. In fact, our measurement is about 33% lower than that of ref. [37]. The theoretical result of Kirby and Cooper [2] is about 31% lower than the present result and agrees with the result of Stark et al. [8], while the value of Lee and Guest [17] is 3.9 times smaller than ours. Our value is also about 1.9 times larger than the measurement of Letzelter et al. [10]. However, the $F(0)$ band is subject to pressure saturation effect. Therefore, the values of the oscillator strengths reported by ref. [17] and ref. [10] for the $F(0) \rightarrow X^1\Sigma^+$ transition may well be affected by pressure saturation effects.

The values of the oscillator strength found here may have important implications for models of CO photodestruction in the ISM. Letzelter et al. [10] have measured the set of absorption cross sections used for modeling CO absorption at photon energies below the Lyman continuum threshold. The data of Letzelter et al. [10] for the singlet state Rydberg series are used as a benchmark for CO photodestruction [1]. A factor of two increase in photodissociation yield of the largest single contributor to predissociation for this molecular state needs to be considered in future ISM modeling.

ACKNOWLEDGMENTS

The research here described was carried out at the Jet Propulsion Laboratory, California Institute of Technology. The work was supported by the U. S. Air Force Office of Scientific Research (AFOSR), the Aeronomy Program of the National Science Foundation (ATM-9320589) and NASA Planetary Atmospheres, Astronomy/Astrophysics, and Space Physics Program Offices. M. Ciocca is supported by the National Research Council through a Resident Research Associateship at the Jet Propulsion Laboratory. The authors also wish to thank W. Ubachs and F. Rostas for valuable discussions and suggestions, and J. Kendall for a careful reading of the manuscript.

REFERENCES

- [1] E.F. van Dishoek and J. H. Black, *Astrophys. J.* 334,771 (1988).
- [2] K. Kirby and D. L. Cooper, *J. Chem. Phys.* 90, 4895(1989).
- [3] Y. P. Viala, C. Letzelter, M. Fidelsberg and F. Rostas, *Astron. Astrophys.* 193,265 (1988).
- [4] E.F. van Dishoek and J. H. Black, in *Physical Processes in Interstellar Clouds*, edited by G. H. Morfill and M. Scholer (Reidel, New York, 1987), p.241.
- [5] M. Fidelsberg and F. Rostas, *Astron. Astrophys.* 235,472 (1990)
- [6] M. Fidelsberg, J. J. Benayoun, Y. Viala, and F. Rostas, *Astron. Astrophys. Suppl.* 90,231 (1991)
- [7] G. Stark, K. Yoshino, P. L. Smith, K. Ito and W. H. Parkinson, *Astrophys. J.* 369,574 (1991).
- [8] G. Stark, P. L. Smith, K. Ito and K. Yoshino *Astrophys. J.* 395,705 (1992).
- [9] G. Stark, K. Yoshino, P. L. Smith, J. R. Fidsmond, K. Ito and M. Stevens, *Astrophys. J.* 410, 837 (1993).
- [10] C. Letzelter, M. Fidelsberg, F. Rostas, J. Breton and B. Thieblemont, *Chem. Phys.* 114,273 (1987).
- [11] M. Drabbels, J. Heinze, J. J. ter Meulen and W. L. Meerts, *J. Chem. Phys.* 99,5701 (1993).
- [12] P. Cacciani, W. Hogervorst, and W. Ubachs, *J. Chem. Phys.*, 102,8308, (1995)
- [13] W. Ubachs, P. C. , P. Hansen, W. Hogervorst and P. Cacciani, *J. Mol. Spectrosc.*, 174,388 (1995)
- [14] D. C. Norton and L. Noreau, *Astrophys. J. Suppl.*, 95,301 (1994)
- [15] I. Kanik, G. K. James and J. M. Ajello, *Phys. Rev. A*, **51**, 2067 (1995).

- [16] F.F. van Dishock, in *Astrochemistry*, edited by M. S. Vardya and S.P. Tarafdar (Reidel, Dordrecht, 1987), p. 51,
- [17] L.C.Lee and J. A. Guest, *J.Phys.B*, 14,3415 (1981)
- [18] W. Ubachs, K. S. E. Fikema, P. Levelt and W. Hogervorst, and M. Drabbels, W. I. Meerts and J. J. Ter Meulen, *Astrophys. J.*, 427,1,55, 1994
- [19] J. Ajello, G. K. James, and B. O. Franklin, *Phys Rev. A*, 40,3524 (1 989)
- [20] G. K. James, J. M. Ajello, I. Kanik, B. O. Franklin, and D. Shemansky, *J. Phys B* 25, 1481 (1 992)
- [21] D. E. Shemansky, J. M. Ajello and D. 'I'. Hall, *Astrophys. J.*, 296,765, (1985)
- [22] D. E. Shemansky, J. M. Ajello, D. 'I', Hall and B. O. Franklin, *Astrophys. J.*, 296,774, (1985)
- [23] X. Liu, S. M. Ahmed, R. Multari, G. K. James, and J. M. Ajello, *Astrophys. J. Supp.*, **101**, 375 (1995).
- [24] J. J. Hopfield and R. T. Birge, *Phys. Rev* 29,922 (1 927).
- [25] R. J. Kelly, "Atomic and Ionic Spectrum Lines below 2000 Angstroms: Hydrogen through Krypton", *J. Chem. Ref. Data*, **16**, Suppl. 1, 1987
- [26] M. Feldsberg, J. -Y. Roncin, A. LeFloch, F. Launay, C. Letzelter and J. Rostas, *J. Mol. Spectrosc.* 121,309,1987
- [27] K. P. Huber and G. Herzberg, "Molecular Spectra and Molecular Structure: IV. Constants of Diatomic Molecules", Van Nostrand, New York (1 979)
- [28] J. D. Simmons and S. G. Tilford, **49**, 167(1974)

- [29] J. Baker, J. L. Lemaire, S. Couris, A. Vient, D. Malmasson, and F. Rostas, Chem. Phys. **178**, S69, (1993).
- [30] G. K. James, J. M. Ajello, I. Kanik, B. O. Franklin, and D. Shemansky, J. Phys B **23**, 2055 (1990)
- [31] J. M. Ajello, D. Shemansky, T. L. Kwok and Y. L. Yung, Phys. Rev. A, **29**, 636, (1984)
- [32] I. Kanik, M. Ratliff, and S. Trajmar, Chem. Phys. Lett., **208**, 341 (1993).
- [33] D. E. Shemansky, and I. Kanik and J. M. Ajello, Astrophys. J., **452**, 480, 1995
- [34] G. Herzberg, "Molecular Spectra and Molecular Structure: I. Spectra of Diatomic Molecules", Krieger Publishing, Malabar, Florida (1989)
- [35] H. A. Bethe, Ann. Phys. (N. Y.) **5**, 325 (1930)
- [36] W. F. Chan, G. Cooper and C. E. Brion, Chem. Phys., **170**, 123 (1993)
- [37] E. N. Lassettre and A. Skerbele, J. Chem. Phys. **54**, 1597 (1971)

FIGURE CAPTIONS

Figure 1 : Partial potential energy curve diagram, emphasizing the 9,5 -12,5 eV region . Shown are the potential energy curves of the levels of CO studied in this work and the Franck-Condon region.

Figure 2: Schematic of Σ - Σ and Σ -1 Σ ICO transitions presented in this work. The quantities η_p^+ and η_p^- are defined in the text.

Figure 3: High resolution (0.036 Å FWHM with 8 mÅ step size) electron-impact induced fluorescence spectrum of CO at 100 eV. The spectrum was obtained at a background pressure of 1.0×10^{-5} Torr. P and R branches are resolved for the C(0, 0) and B(0, 0) transitions, but only the Q branch appears for the E(0, 0).

Figure 4: Comparison between data and model for the B $^1\Sigma^+(0) \rightarrow$ X $^1\Sigma^+(0)$ transition. The rotational line intensities in the model, based on the Hönl-London factors and the unperturbed rotational constants of Ubachs et al. [18], reported in Table I, have been convoluted with a triangular response function (0.036 mÅ FWHM). Indicated are the first few rotational lines of each branch.

Figure 5: Comparison between data and model for the C $^1\Sigma^+(0) \rightarrow$ X $^1\Sigma^+(0)$ transition. The rotational line intensities in the model, based on the Hönl-London factors and the unperturbed

rotational constants of Ubachs et al. [18] reported in ‘Table 1, have been convoluted with a triangular response function (0.036 mÅ FWHM). Indicated are the first few rotational lines of each branch.

Figure 6: Comparison between data and model for the $B^1\Pi(0) \rightarrow X^1\Sigma^+(0)$ transition. The rotational line intensities in the model, based on the Hönl-London factors and the unperturbed rotational constants of Eidelsberg et al. [5], reported in ‘Table I, and with a ratio of 0.63 between the Qbranch(Π State) the P and R Branch (Σ State) predissociation yields, have been convoluted with a triangular response function (0.036 mÅ FWHM).

Figure 7: Relative emission cross section (excitation function) of the $COE^1\Pi(0,0)$ band at 1076.1 Å in the range 0-800 eV electron impact energy.

Figure 8: Model fit for the excitation (curve a), predissociation (curve b), emission (curve c) and branching (curve d) cross sections for the $COE^1\Pi(0)$ state. Emission and branching cross sections are multiplied by a factor of 5.

Figure 9: Model and data of the collision strength of the $COE^1\Pi(0,0)$ band plotted against energy (1 0-800 eV). The oscillator strength (f value) for this feature is determined as 7.08×10^{-2} .

LIST OF TABLES

TABLE I: Constants used in the Model Spectra

TABLE II: Excitation, emission, predissociation and branching cross section of CO($v=1$) at 100 eV

TABLE III: Constants of the Modified Born equation

TABLE IV: Summary of previous and present determinations of oscillator strength between the CO($v=1$) state and the ground state X($v=0$).

TABLE 1

Constants Used in the Model Spectra: all values in cm⁻¹

Slate	v_0	B_v	D_v	Rcf
B $^1\Sigma^+$ (o)	86916.1581	1.948173	6.90X 106	a
C $^1\Sigma^+$ (o)	91919.0719	1.943425	6.172X10 ⁴	a
E $^1\Pi$ (o)	92929.98	1.95261	6.50X 10<	b
x $^1\Sigma^+$ (o)		1.92253	6.11948x10 ⁻⁶	c

a) W. Ubachs et al. [18]

b) M. Fidelsberg et al. [5]

c) Huber and Herzberg [27]

TABLE 11

Cross Sections at 100 eV for the CO²⁺ 1 (0) state (all values in cm² x 10⁻¹⁸).

Q_{exci}	=	4.43
Q_{emis}	=	0.47
Q_{pre}	=	3.91
Q_{b}	=	0.038

TABLE III

Constants of the Modified Born equation(*)

\mathbf{I}	$\mathbf{E(II)}$
C_0	0
C_1	-0.11229
C_2	0.58790
C_3	-1.7784
C_4	1.8675
C_5	-0.35586
C_6	0.35586
C_7	0.33437
C_8	0.26915

(* Modified Born Equation:

$$\Omega_{v^m} (X_{v^m}) = C_0 (1-1/X_{v^m}) (X_{v^m}{}^2) + \sum_{k=1}^4 C_k (X_{v^m}{}^k - 1) \cdot \exp(-k \cdot C_8 \cdot X_{v^m}) + C_5 + C_6 / X_{v^m} + C_7 \cdot \ln(X_{v^m})$$

TABLE IV

Summary of previous and present determination of oscillator strength $f_{\nu'\nu''}$ ($\times 10^{-2}$) for the transition between the COE ${}^1\Pi(0)$ state and the ground state $X\ {}^1\Sigma^+(0)$.

Source	f_{00}
Kirby and Cooper (theory) [2]	4.9
Stark et al. [8]	4.9
Metzelter et al. [10]	3.65
Lee and Guest [17]	1.81
Chan et al. [35]	7.06
Lassetre and Skerbele [36]	9.40
This work	7.08

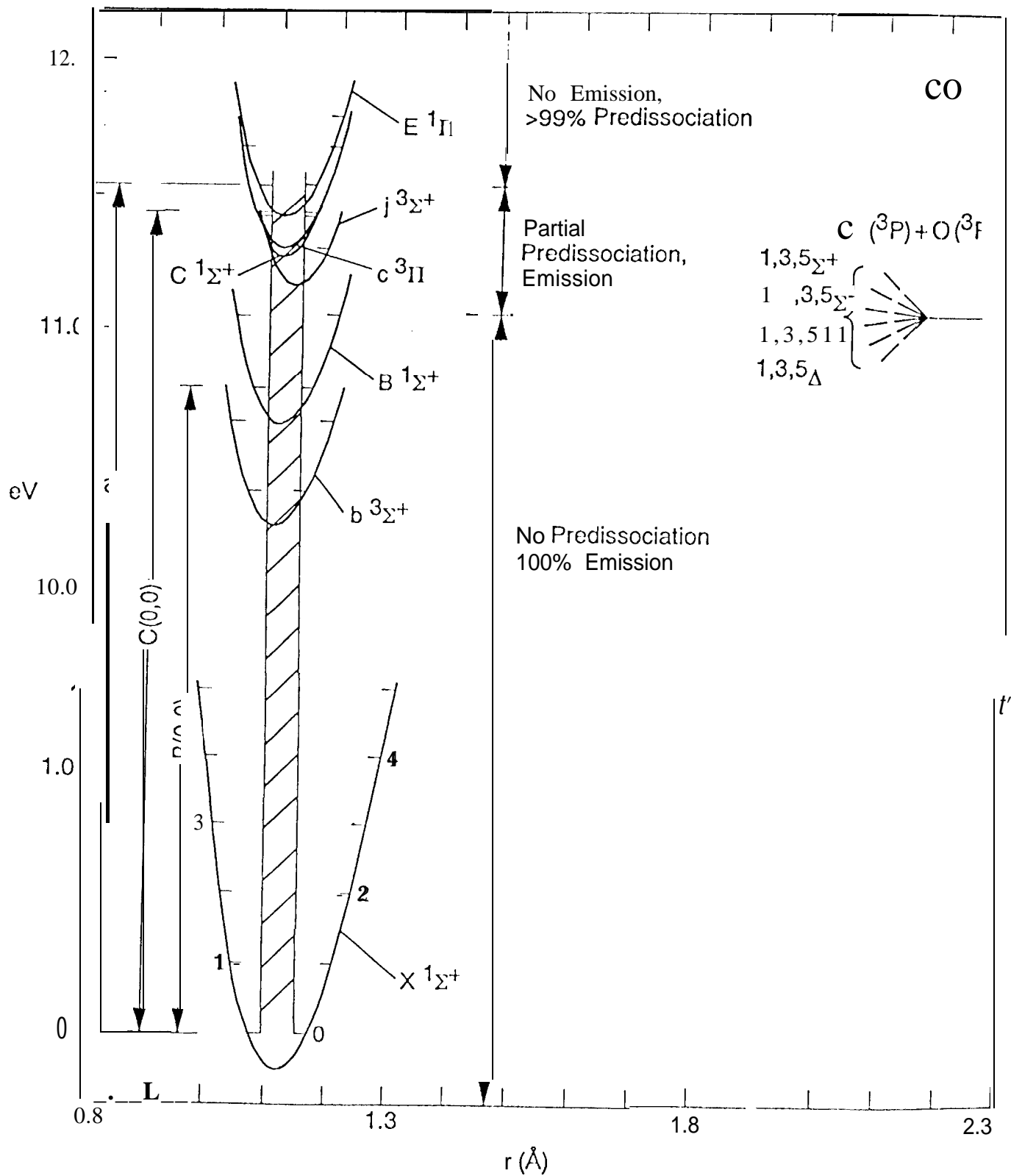


Fig. 1

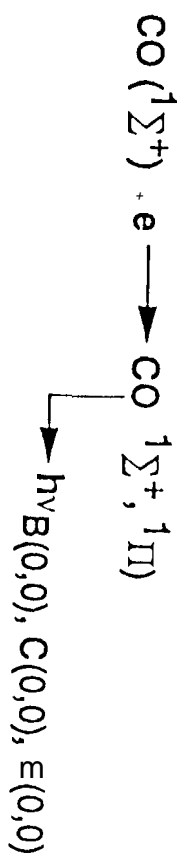
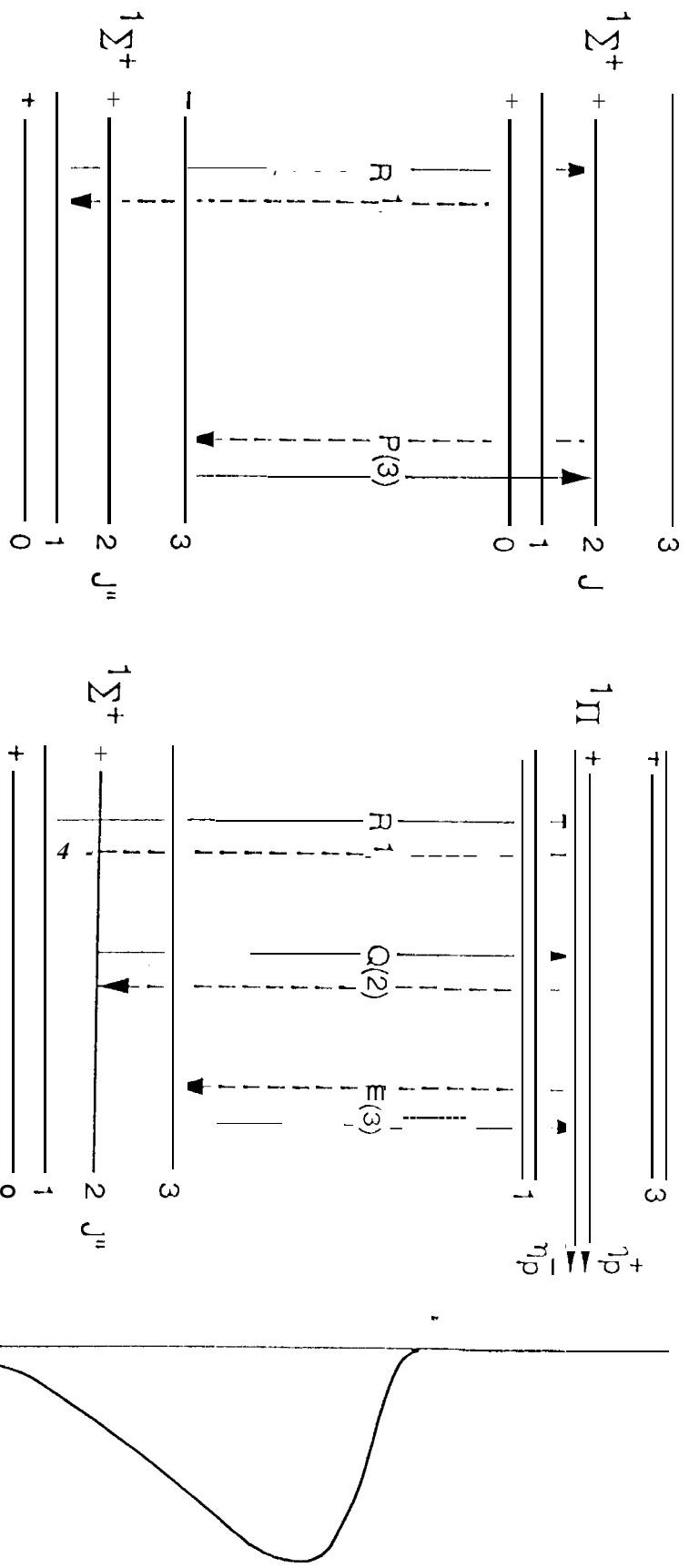


fig 2

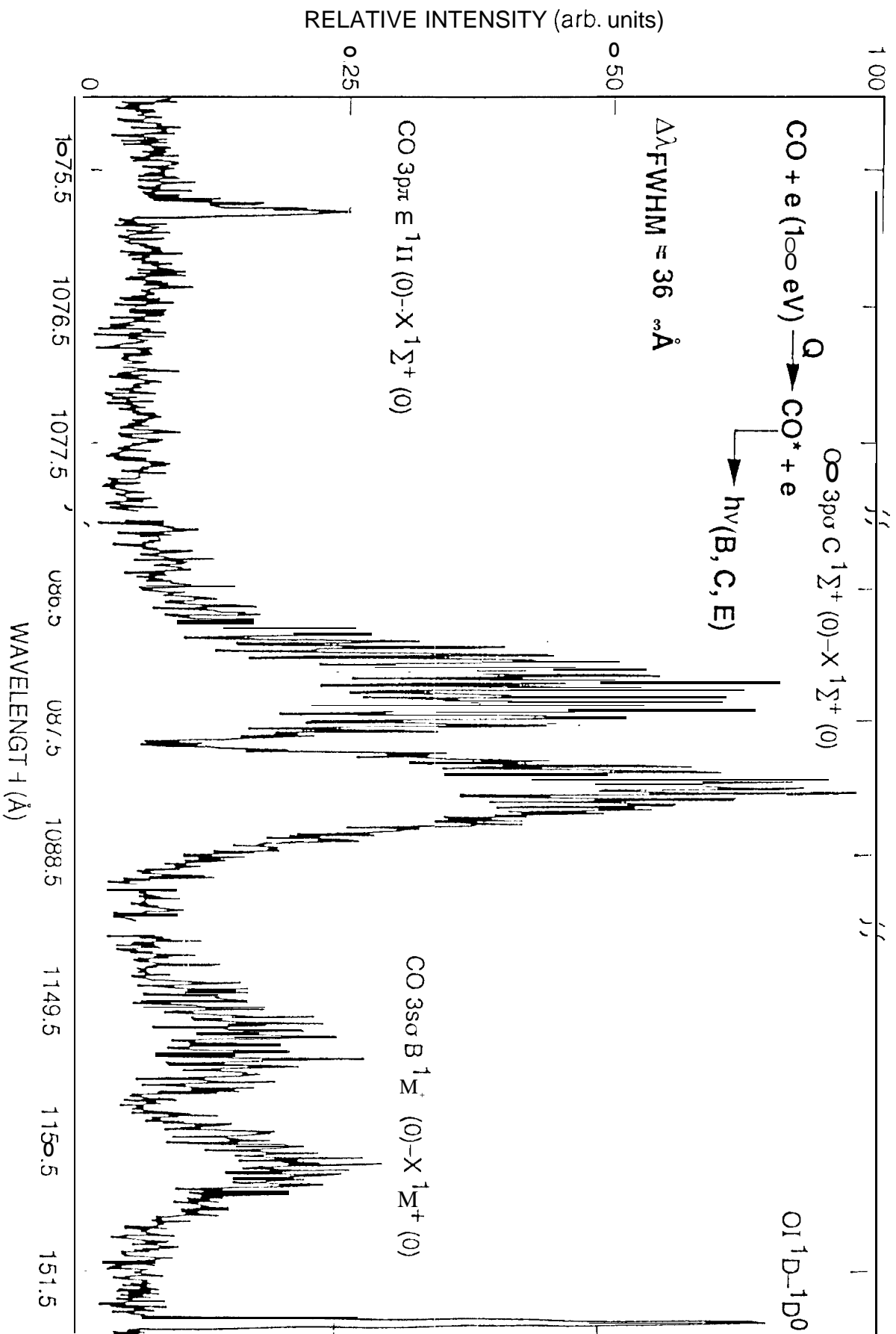


fig 3

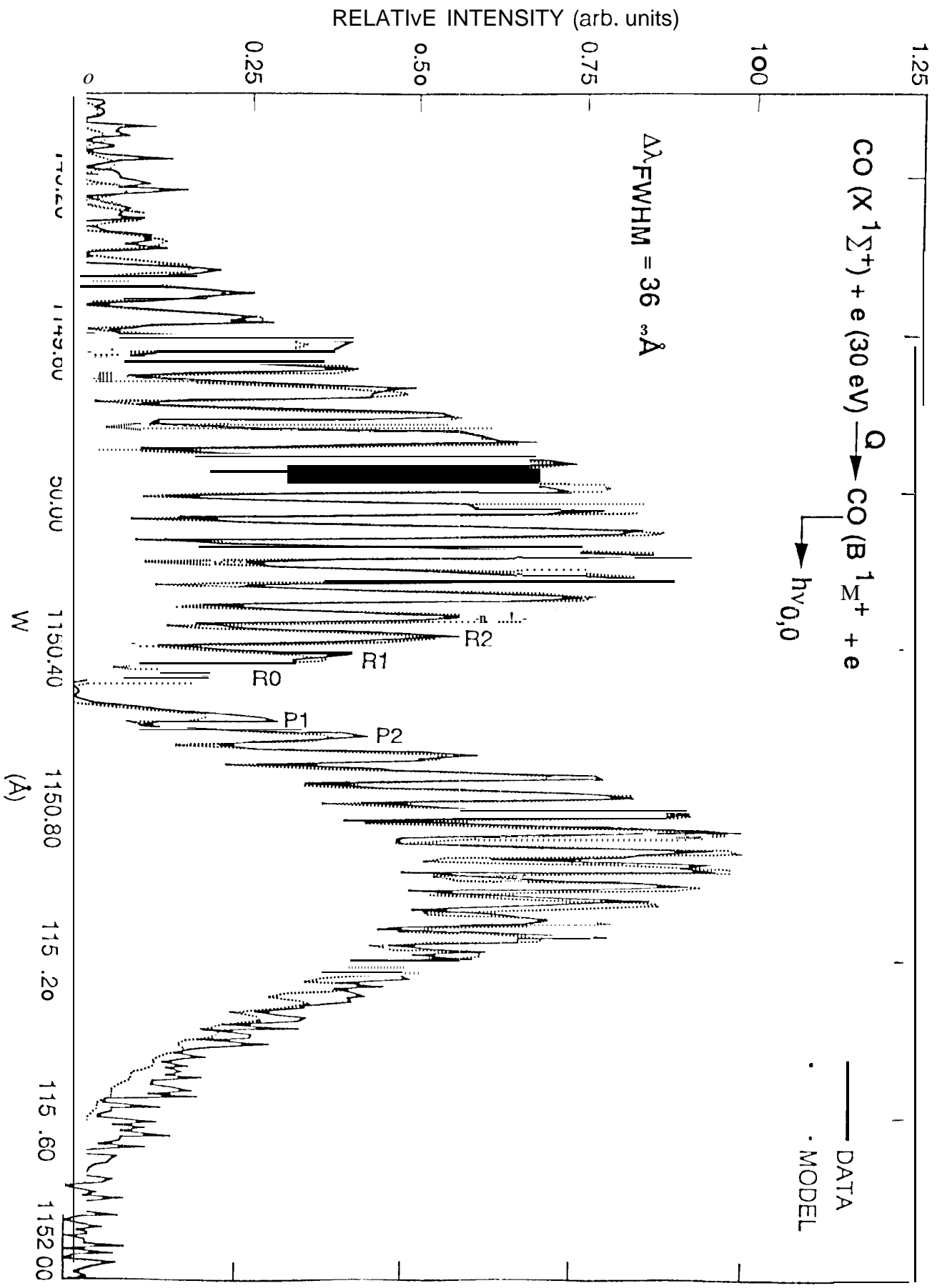


fig 4

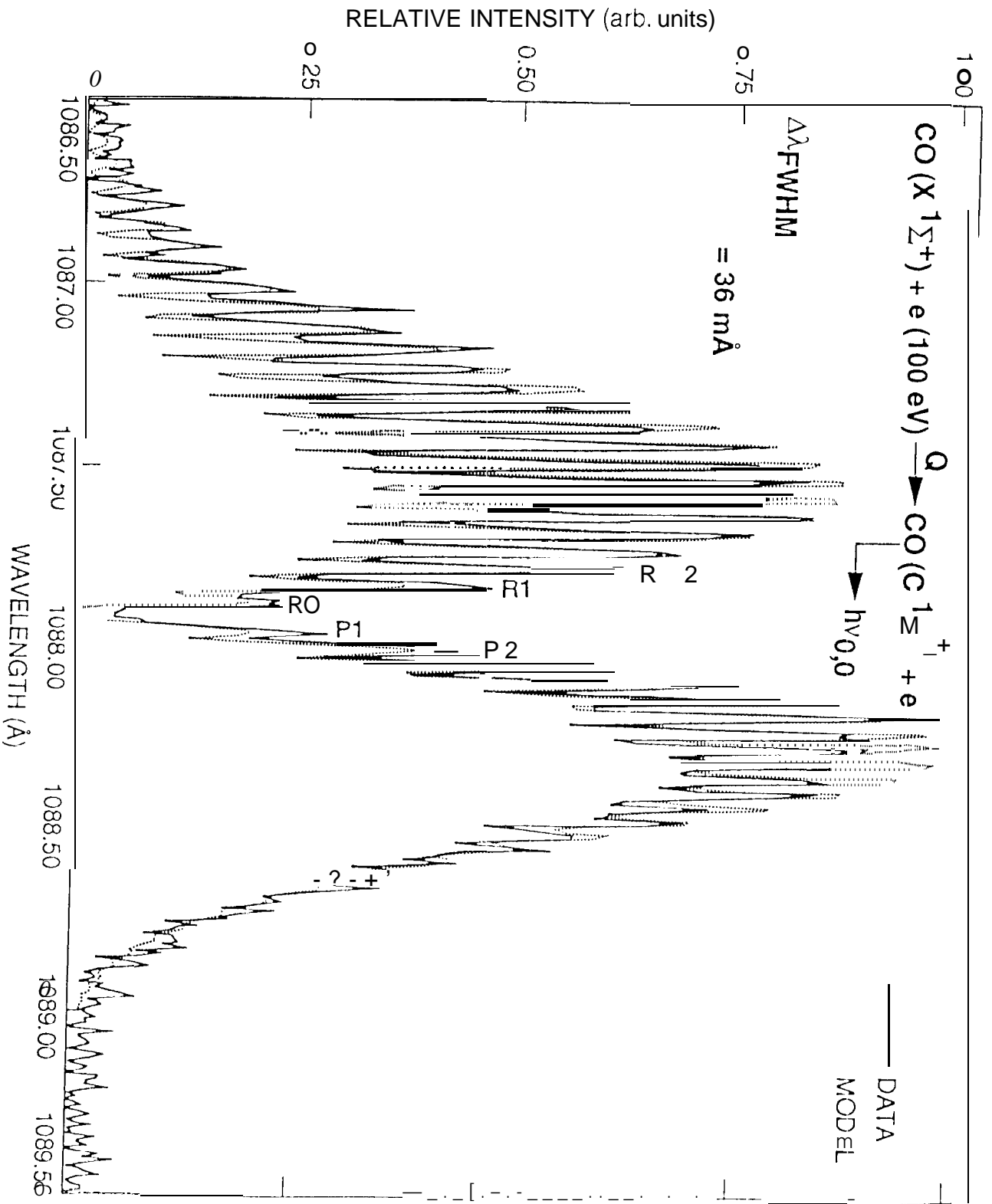


Fig. 5

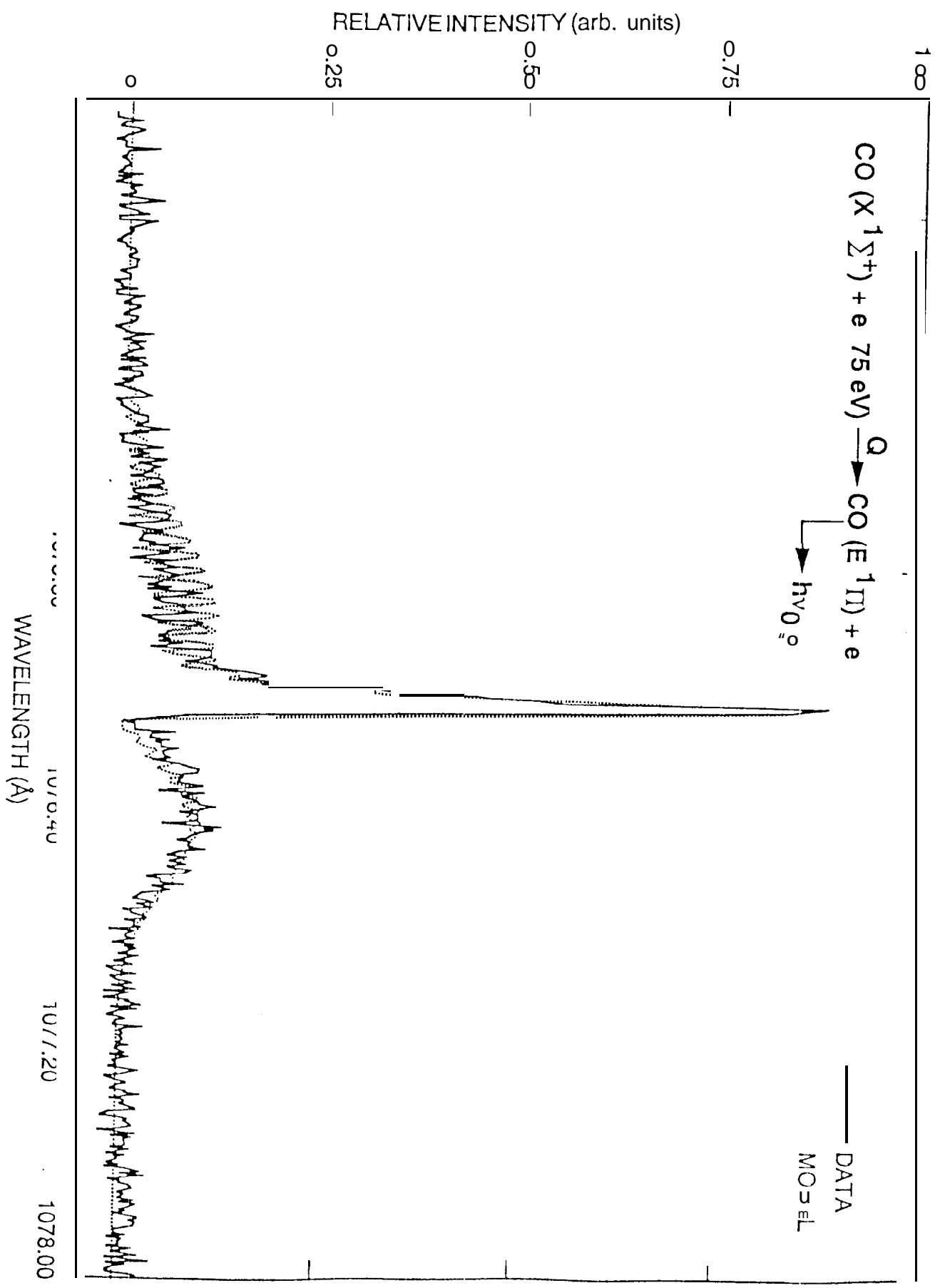


Fig. 6

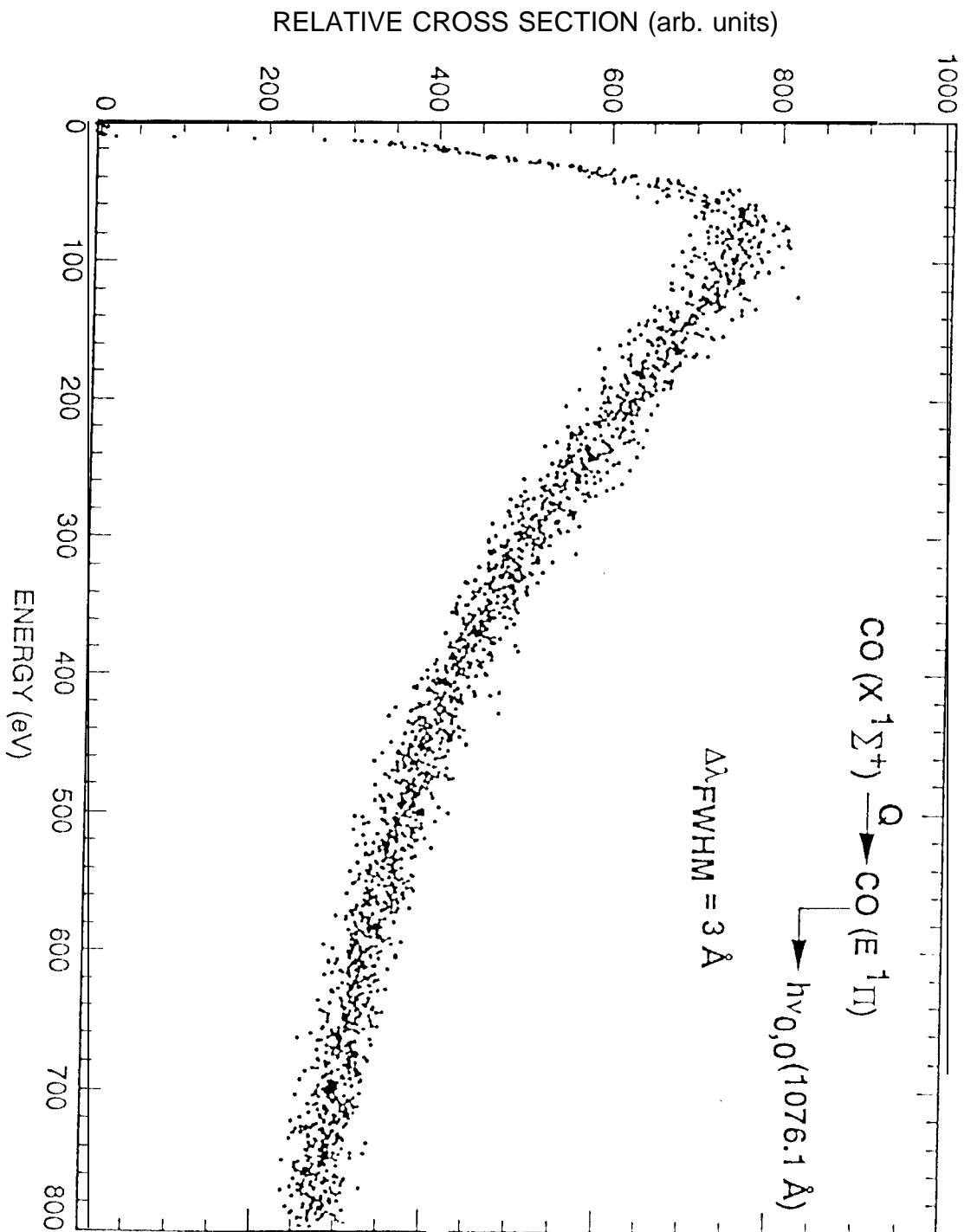


fig 7

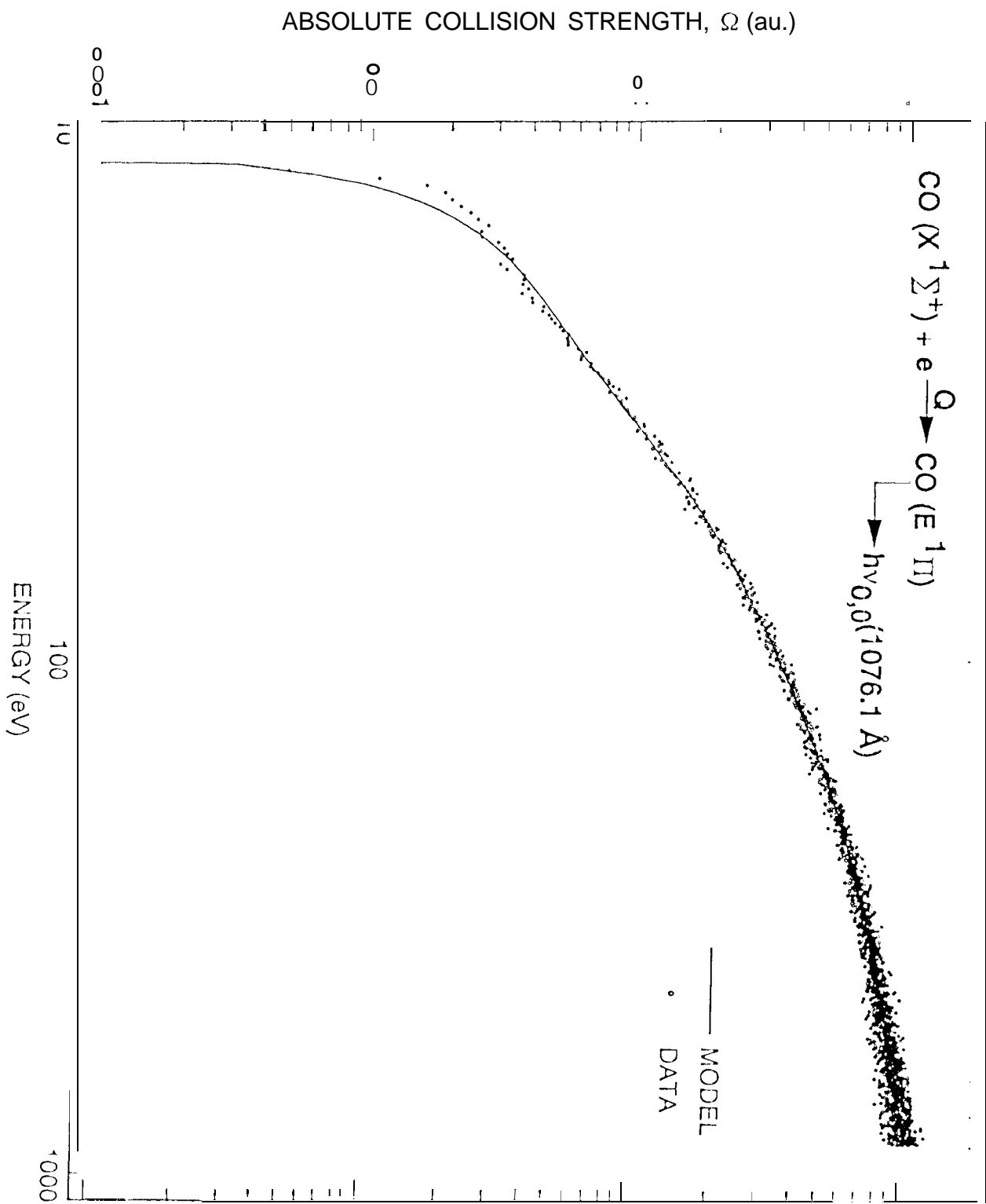
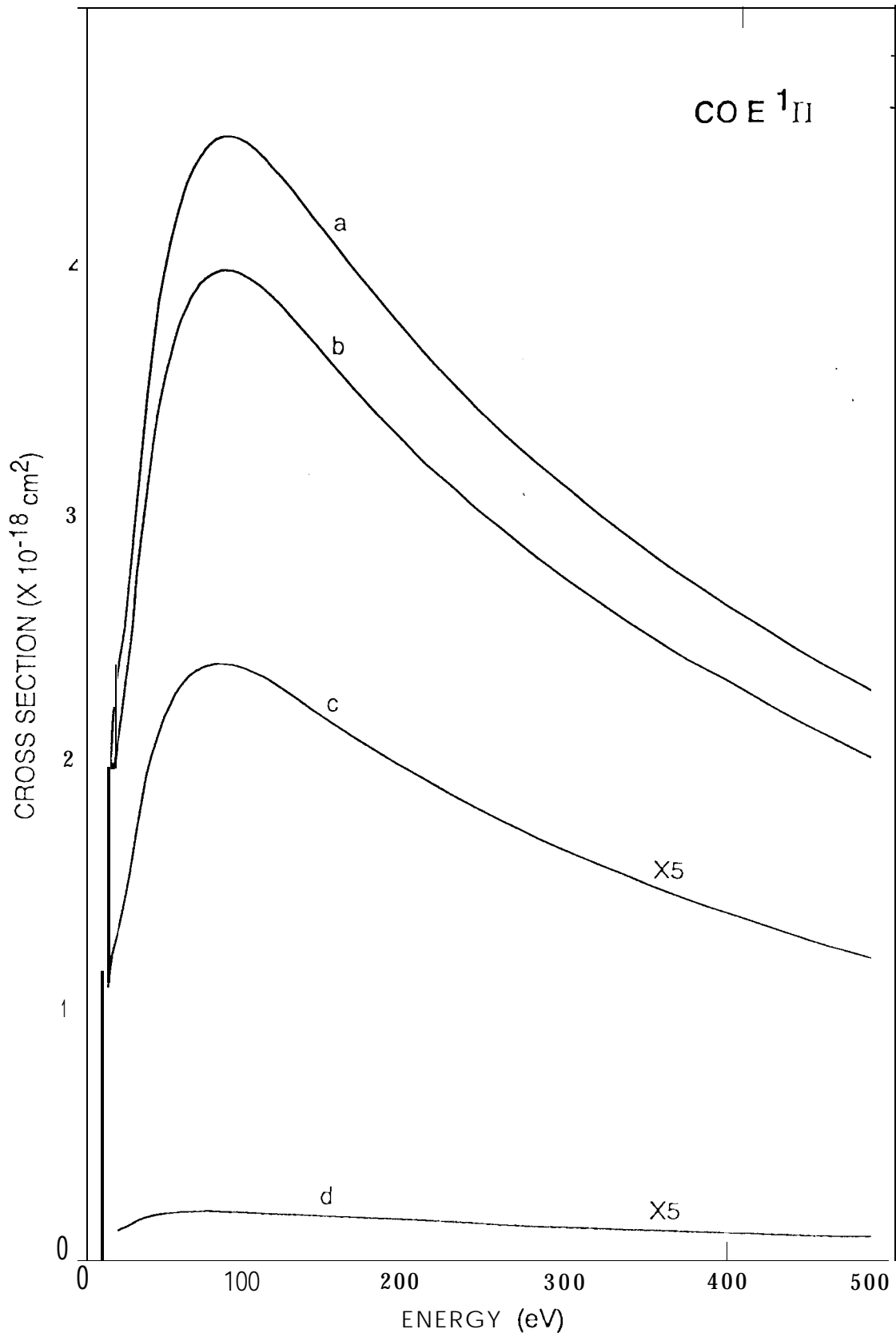


Fig. 8



F-fig. 9